'Ab Initio' Calculations on Methane Interacting with the Fourteen-electron $Ni(PH_3)_2$ Fragment†

Nazzareno Re,[a] Marzio Rosi,[a] Antonio Sgamellotti,*[,a] Carlo Floriani[b] and Martyn F. Guest[c]

[a] *Dipartimento di Chimica, Università di Perugia, Via Elce di Sotto 8, I-06100 Perugia, Italy*
[b] *Section de Chimie, Université de Lausanne, Place du Château 3, CH-1005 Lausanne, Switzerland*
[c] *SERC Daresbury Laboratory, Daresbury, Warrington WA4 4AD, UK*

Ab initio restricted Hartree–Fock and configuration interaction calculations have been carried out on the system $Ni(PH_3)_2 + CH_4$ in order to study the energetics and the mechanism of the oxidative-addition reaction of CH_4 and to model the activation of the C–H bond by zerovalent, co-ordinatively unsaturated transition-metal complexes. Energy-gradient optimizations and transition-state localizations have been performed on reactants and products in various constrained geometries. The results indicate that the oxidative addition of methane to $Ni(PH_3)_2$ is endothermic by 7.0 kcal mol^{-1} and the planar *trans* product is the most stable, being lower in energy than the *cis* isomer by 3.4 kcal mol^{-1}.

The activation of C–H bonds by metal complexes has recently drawn much interest in view of the development of catalytic routes to alkane functionalization.[1–5] The unreactivity of the alkanes, due both to the strong bonding between C and H (dissociation energy in the range 90–100 kcal mol^{-1}) and to the low polarity of the C–H bond, makes their activation a challenging problem. Although faced since the early 1960s,[6,7] significant advances in understanding the factors influencing the reactivity of the C–H bond[8–12] and the model complexes to be used for such a purpose have been made only in recent years.

The C–H bond activation pathways are essentially three:[2,3] oxidative addition, homolytic and heterolytic cleavage of the bond. Among them, the most studied mode of activation is, from a theoretical point of view, oxidative addition, though this was mainly in the past approached with the extended-Hückel formalism. The *ab initio* calculations should provide an increasing contribution to the theory of C–H bond activation. An *ab initio* approach to the C–H bond oxidative addition to nickel(0) is exemplified in this paper [reaction (1)]. It is well

$$'(H_3P)_2Ni' + CH_4 \longrightarrow (H_3P)_2NiH(CH_3) \qquad (1)$$

known that such a reaction is favoured when the metal complex has a low-energy empty σ-type molecular orbital (MO) able to accept the C–H bonding pair and a high-energy MO containing the lone pair which will be transferred to the empty σ* orbital of the C–H bond.

Although appealing such an activation mode by a metal centre has two main drawbacks. (*a*) Reaction (1) is usually thermodynamically unfavoured due to the relative weakness of the M–H and M–C bonds; as a consequence oxidative addition is possible only for highly unstable low-valent and co-ordinatively unsaturated complexes.[8,9] (*b*) The H^- and $\equiv C^-$ ligands remain in the same co-ordination sphere of the central metal and may easily give rise to reductive elimination, *i.e.* to the reverse of equation (1). As the reductive elimination is usually thermodynamically favoured (and in fact alkane reductive elimination is a fairly common process in organometallic chemistry,[13] much more than the alkane oxidative addition) any attempt to produce subsequent reactions of the C or H ligands leads almost invariably to reductive elimination and therefore to the original alkane.

Both the energetics and mechanism of reaction (1) have been approached with *ab initio* methods. Then we took the following steps: (*i*) for the final product of reaction (1) three different structures, *cis*-planar, *trans*-planar and tetrahedral were considered; (*ii*) a study has been performed on the $Ni(PH_3)_2{\cdot}CH_4$ adduct, methane displaying an end-on, pseudo-side-on or bifurcated bonding mode, with a partial investigation of the energy profile connecting these complexes with the final products of the oxidative addition; (*iii*) an attempt has been made to relate this latter study to the problem of the so-called 'agostic' interaction between a C–H bond and a metal centre.[3,14–16]

Computational Details

Basis Set.—The s,p basis for nickel was taken from the 12s6p4d set of ref. 17 with the addition of two basis functions to describe the 4p orbital,[18] while the nickel d basis was the reoptimized (5d) set of ref. 19, contracted (4/1). This leads to an (11s8p5d) primitive basis for nickel, contracted (8s6p2d). The MINI-1[20] basis was used for the phosphorus atoms, while a double ζ expansion was used for all the other ligand atoms, with a (4s/2s) basis for hydrogen[21] and a (9s5p/4s2p) contraction for carbon.[21]

Methods.—The calculations have been performed at two levels of accuracy. The linear combination of atomic orbitals (LCAO)–self consistent field (SCF)-MO scheme has been employed to derive ground-state energies and wavefunctions for all the investigated structures and to perform the various geometry optimizations and transition-state calculations. Single reference-state single-plus-double configuration interaction (SDCI) calculations were subsequently performed on some of the stationary points determined at the SCF level. These calculations have been performed with the direct CI method,[22] limiting to the single-reference SDCI since no configurations with a coefficient greater than 0.04 were present in the SDCI wavefunction. To reduce the size of the CI problem (37 doubly occupied orbitals and 86 basis functions) for the $[Ni(PH_3)_2(CH_3)H]$ complex, 40 inner electrons have been frozen. In the corresponding SDCI calculations on the $Ni(PH_3)_2$ and CH_4 fragments we froze the orbitals correlating

† *Non-SI units employed:* cal = 4.184 J, Hartree (E_h) ≈ 4.36 × 10^{-18} J.

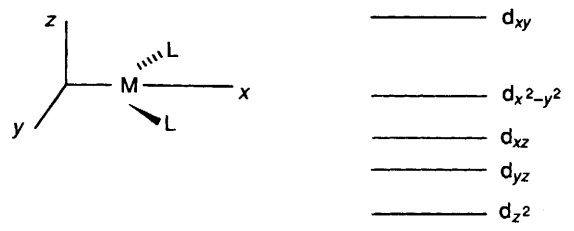

Fig. 1 d-Orbital levels for a ML_2 complex

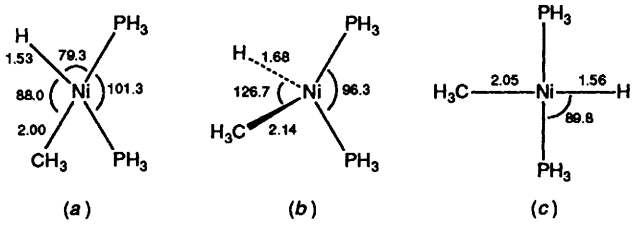

Fig. 2 Optimized geometries for (*a*) *cis*-planar, (*b*) tetrahedral and (*c*) *trans*-planar structures. Bond lengths in Å, angles in °

Table 1. Total and metal fragment SCF energies[a] for the planar, *cis* and *trans*, and tetrahedral $[Ni(PH_3)_2(CH_3)H]$ complexes, and corresponding binding energies (b.e.s). The units used are Hartree (E_h) for the total energies and kcal mol^{-1} for the binding energies

	Planar *cis*	Planar *trans*	Tetrahedral
$E_{complex}$	−2227.9274	−2227.9508	−2227.8813
$E^{b}_{fragment}$	−2187.7138	−2187.7438	−2187.7193
b.e.[c]	+1.3	−13.3	+32.4
b.e.[d]	−17.5	−13.3	+13.6

[a] For methane $E = -40.1856$ E_h. [b] Metal fragment in the same geometry as in the corresponding optimized complex. [c] Referred to the metal fragment in the optimized linear geometry ($E = -2187.7439$ E_h). [d] Referred to the metal fragment in the same geometry as in the corresponding optimized complex.

with those frozen for the complex. The Davidson correction[23] was made for the lack of size consistency of the wavefunction.

All computations were performed by using the GAMESS program package,[24] implemented on a IBM 3090 VEC computer.

With regard to the characterization of the ground state, we have assumed an A_{1g} singlet state for the methane, as experimentally well known, and a closed-shell singlet also for the $Ni(PH_3)_2$ fragment and the $Ni(PH_3)_2$·CH_4 adducts. The ground states of these latter zerovalent nickel complexes are considered to be closed-shell singlets of d^{10} character,[25] although in the free nickel atom the lowest electronic states $^3D(3d^94s^1)$, $^3F(3d^84s^2)$ and $^1S(3d^{10})$ lie energetically close to each other. The assumed $3d^{10}$ electronic configuration is justified by the consideration that the presence of the two PH_3 ligands should destabilize the more diffuse 4s and 4p orbitals to a larger extent than the 3d orbitals and by some recent calculations on other zerovalent nickel complexes.[26–28] We have assumed a closed-shell singlet configuration also for the d^8 $[Ni(PH_3)_2(CH_3)H]$ complex on the basis of the schematic representation of the d-orbital levels for a d^8 metal in a square-planar field (see Fig. 1).

Geometry and Geometry Optimization.—In all the calculations we have assumed for the $Ni(PH_3)_2$ fragment a Ni–P bond length of 2.198 Å which is an average value of various $Ni(PR_3)_2$ complexes[29] and for the PH_3 ligand the geometry of free PH_3.[30] The geometry utilized for the methane and the methyl group is that obtained in the complete geometry optimization of the methane itself, unless differently stated.

For the oxidative-addition product $[Ni(PH_3)_2(CH_3)H]$ we have performed geometry optimizations on the two planar and pseudo-tetrahedral structures varying five internal coordinates. The P–Ni–P angles obtained in the optimization of the planar structures, which are much lower in energy than that of the tetrahedral one, have been utilized in the subsequent geometry optimizations of the $Ni(PH_3)_2$·CH_4 adducts in various conformations (end-on, pseudo side-on, bifurcated and others). All the geometry optimizations have been performed using the quasi-Newton procedure available in the GAMESS package.[24]

Transition-state calculations were performed in order to determine the reaction coordinate connecting the $Ni(PH_3)_2$·CH_4 adduct in the energetically lowest conformation with the optimized planar $[Ni(PH_3)_2(CH_3)H]$ complex. They have been performed using a modified variant of the synchronous transit algorithm available in the GAMESS package.[24]

Results and Discussion

Oxidative Addition.—The $[Ni(PH_3)_2(CH_3)H]$ complex obtained by the oxidative-addition reaction (1) has been investigated in the planar (*cis* or *trans*) and pseudo-tetrahedral structures, both corresponding to C_s symmetry. Three different partial geometry optimizations have been performed with the constraints that the C–Ni–H and P–Ni–P planes were coplanar or perpendicular. In two cases we have optimized five geometrical parameters involving the nickel atom and the methane-derived ligands: Ni–H and Ni–C bond lengths, P–Ni–P and C–Ni–H angles, and H–Ni–P angle for the *cis*-planar structure or the angle between the Ni–H bond and the P–Ni–P plane for the tetrahedral structure. For the *trans*-planar structure we have imposed a C–Ni–H collinear constraint so that we could optimize only three geometrical parameters: Ni–H and Ni–C bond lengths and P–Ni–P angle. The optimized geometries for the three structures are reported in Fig. 2. The corresponding total SCF energies are in Table 1 together with the estimated reaction energies. The SCF energies for the $Ni(PH_3)_2$ and CH_4 separated fragments have been obtained respectively by optimizing the P–Ni–P angle and by complete geometry optimization. For the nickel fragment we obtained an optimized linear structure with a P–Ni–P angle of 180°. As can be seen in Table 1, the tetrahedral structure is much higher in energy than the planar ones and, therefore, only results relative to the planar complexes will be considered. On the other hand, when considering the planar complexes, the SCF energy for the oxidative addition is calculated to be +1.3 kcal mol^{-1} for the *cis* structure and −13.3 kcal mol^{-1} for the *trans* one. This means that, at the SCF level, there is a thermodynamic preference for the *trans* compound over the *cis* one by 14.6 kcal mol^{-1}. However, when we consider the reaction energy with respect to the fragments with the same P–Ni–P angle as that of the optimized final complex, we obtain −17.5 and −13.3 kcal mol^{-1} respectively for the *cis* and *trans* structures: this is due to the higher energy (18.9 kcal mol^{-1}) of the bent fragment (P–Ni–P 101.3°) in the *cis* geometry with respect to the almost linear fragment (P–Ni–P 179.7°) in the *trans* geometry.

A characterization of the binding features of the methane-derived ligands in the $[Ni(PH_3)_2(CH_3)H]$ complexes can be attempted on the basis of an analysis of the frontier molecular orbitals of the complex and of the separated fragments. We consider first the *cis*-planar complex. In the corresponding $Ni(PH_3)_2$ bent fragment the highest-occupied molecular orbital (HOMO) is mainly a nickel d_{xy} orbital as predictable by simple ligand-field considerations (see Fig. 1). The lowest unoccupied molecular orbital (LUMO) is mainly a hybridized $s–p_x–p_y$ orbital directed to the opposite side of the PH_3 ligands. These HOMO and LUMO interact with bonding and antibonding combinations of the 1s orbital of hydrogen and of the hybridized s–p orbitals of the CH_3 group, respectively, in order to give the two lowest-occupied orbitals of the $[Ni(PH_3)_2(CH_3)H]$ complex. As a consequence there is an increase in electron density in

Table 2 Mulliken population changes for *cis*- and *trans*-planar $[Ni(PH_3)_2(CH_3)H]$ complexes

	cis	*trans*
Ni	−0.45	−0.57
Ni s	+0.24	−0.02
Ni p	+0.24	+0.36
p_x	+0.15	0.00
p_y	+0.09	+0.28
p_z	0.00	+0.08
Ni d	−0.91	−0.95
$d_{x^2-y^2}$	−0.19	−0.30
d_{z^2}	+0.07	−0.75
d_{xy}	−0.88	+0.05
d_{xz}	+0.04	−0.02
d_{yz}	+0.04	+0.06
$2PH_3$	−0.28	−0.20
H	+0.46	+0.50
CH_3	+0.28	+0.28

Table 3 Nickel Mulliken population for *cis*-planar $[Ni(PH_3)_2(CH_3)H]$ complexes and the corresponding bent fragment

	cis Complex	Fragment
Ni	27.43	27.89
Ni s	6.31	6.08
Ni p	12.36	12.12
Ni d	8.77	9.68

Table 4 Total and metal fragment CI energies[a] for the *cis*- and *trans*-planar $[Ni(PH_3)_2(CH_3)H]$ complexes, and corresponding binding energies (b.e.s). The units used are Hartree for the total energies and kcal mol^{-1} for the binding energies

	cis	*trans*
$E_{complex}$	−2228.5349	−2228.4453
$E^b_{fragment}$	−2188.2189	−2188.2515
b.e.[c]	+10.4	+7.0
b.e.[d]	−10.1	+7.0

[a] For methane $E = -40.2999\ E_h$. [b] Metal fragment in the same geometry as in the corresponding optimized complex. [c] Referred to the metal fragment in the optimized linear geometry ($E = -2188.2516\ E_h$). [d] Referred to the metal fragment in the same geometry as in the corresponding optimized complex.

the nickel s and p orbitals and a decrease in the d_{xy} orbital, corresponding to σ donation and π-back donation, respectively. This bonding picture is confirmed by the results of a Mulliken population analysis, whose results are reported in Table 2 as population changes, *i.e.* Mulliken population of the complex minus Mulliken population of the fragments. We notice a strong decrease (−0.88) in the population of the nickel d_{xy} orbital and an increase in the population of the nickel s orbitals (+0.24) and p_x and p_y orbitals (+0.24). Another noticeable feature in the Mulliken analysis is the strong increase in the electron density of both the methyl group (+0.28) and the hydrogen directly bound to nickel (+0.46).

When we consider the *trans* complex the binding scheme is somewhat different. In the linear $Ni(PH_3)_2$ the highest molecular orbital is mainly a nickel d_{z^2} orbital with minor nickel s contributions. Lower in energy we have two groups of doubly degenerate orbitals essentially constituted by d_{xz}, d_{yz} and d_{xy}, $d_{x^2-y^2}$ nickel orbitals lying respectively at −0.27 and −0.28 Hartree. Moreover the lowest-unoccupied orbital is degenerate and consists mainly of nickel p_x and p_y orbitals. In *trans*-$[Ni(PH_3)_2(CH_3)H]$ the two lowest-occupied orbitals can be considered as arising from the interaction of nickel p_y and $d_{y^2-z^2}$ orbitals with bonding and antibonding combinations of the 1s orbital of hydrogen and hybridized s–p orbitals of the CH_3 group, respectively. The highest-occupied orbital in the $Ni(PH_3)_2$ fragment, mainly a nickel d_{z^2}, becomes an unoccupied orbital in the *trans* complex, while one of the two lowest degenerate unoccupied orbitals becomes the higher occupied one. This bonding picture is again confirmed by the Mulliken population analysis (see Table 2), which indicates a relevant decrease in the nickel d_{z^2} population and an increase in the nickel p_y population. As in the *cis* case, we have also a strong increase in the electron density of both the methyl group (+0.28) and the hydrogen directly bound to nickel (+0.50). Both these bonding schemes confirm the usual qualitative interpretation of the C–H bond activation by metal centres through oxidative addition: a forward electron transfer from the bonding σ(C–H) orbital into empty metal orbitals and a backward electron transfer from occupied metal d orbitals into an antibonding σ*(C–H) orbital. However, the reaction cannot be considered a complete oxidation with a transfer of one electron to each, H and CH_3, ligand: the overall charge transfer based on Mulliken population analysis (see Table 2) is only 0.7–0.8 e and not 2 e as it should be for a true oxidative addition. The Ni–C and Ni–H bonds have a substantial covalent character which requires a partial promotion of the metal d-electron density into s and p orbitals, as is shown by the absolute Mulliken population analysis reported in Table 3. In other words, in the oxidative-addition reaction the Ni atom undergoes a promotion from a d^{10} to a $(sp)^1d^9$ configuration rather than a real charge transfer to a d^8 configuration: this is in good agreement with the results of other theoretical investigations on analogous systems of Pd and Pt.[31–34]

Since from our SCF analysis small energy differences have been found between the starting and the final complex of the oxidative addition of CH_4 to $Ni(PH_3)_2$, correlation effects may play an important role and even reverse the energetics of the analysed reaction. Therefore, in order to analyse the effect of the correlation energy on the reaction (1), we have performed SDCI calculations on the *cis*- and *trans*-planar $[Ni(PH_3)_2(CH_3)H]$ complexes at the optimized SCF geometries as well as on the separated fragments. The CI total energies for the planar complexes and the estimated binding energies are reported in Table 4. We notice that the effect of the correlation energy is to destabilize the oxidative-addition product increasing the energy of reaction (1) to +10.4 kcal mol^{-1} for the *cis* product and +7.0 kcal mol^{-1} for the *trans* one. When we consider the reaction energy with respect to the fragments with the same geometry as that of the optimized final complex we obtain at the CI level −10.1 and +7.0 kcal mol^{-1}, respectively, for the *cis* and *trans* structures. Note that at the CI level the *trans* isomer is again the most stable, but the energy difference with the *cis* one is reduced to only 3.4 kcal mol^{-1} (from 14.6 kcal mol^{-1} at SCF level): correlation energy favours the *cis* isomer more than the *trans* one. These results at the CI level indicate that the oxidative addition of methane to $Ni(PH_3)_2$ is thermodynamically disfavoured over the inverse reductive coupling reaction by 7.0 kcal mol^{-1}, and that the planar *trans* product is the most stable. However, if we consider the oxidative addition with a fragment in a bent (P–Ni–P 101.3°) structure, the reaction may be slightly exothermic by 10.1 kcal mol^{-1}. This should be considered as very important information to the chemist on how to generate the fragment and about the ligands and the reaction conditions favouring, depending on the steric hindrance, the geometry of the reactive species.

Methane Complexes and Transition States.—In a preliminary study of the potential-energy surface and of the transition states for the oxidative addition, we have performed various partial geometrical optimizations of the $CH_4 + Ni(PH_3)_2$ system, searching for stationary points corresponding to stable methane complexes. The evidence for a C–H bond acting as a ligand toward an unsaturated metal is well documented in the literature.

In this context a crucial choice was the relative orientation

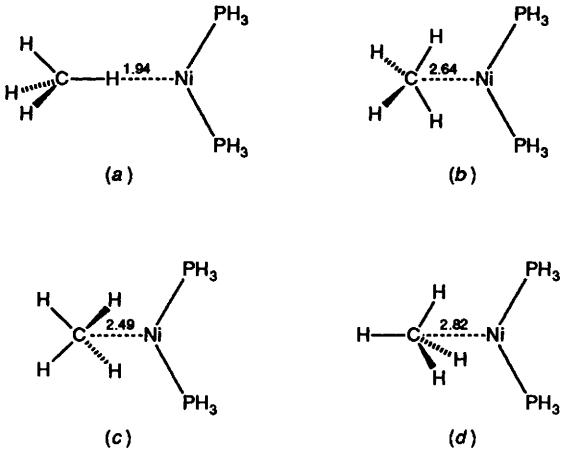

Fig. 3 Optimized geometries for the $Ni(PH_3)_2{\cdot}CH_4$ adduct in (*a*) σ, (*b*) η^2-planar, (*c*) η^2-pseudo-tetrahedral and (*d*) η^3 structures. Bond lengths in Å

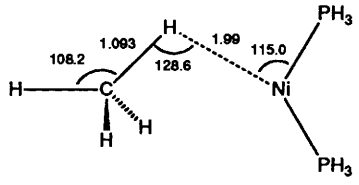

Fig. 4 Optimized geometry for the pseudo-side-on $Ni(PH_3)_2{\cdot}CH_4$ adduct. Bond lengths in Å, angles in °

Table 5 Total SCF energies and corresponding binding energies (b.e.s) for the σ, η^2 (planar and pseudo-tetrahedral) and η^3 $[Ni(PH_3)_2(CH_3)H]$ complexes. The units used are Hartree for the total energies and kcal mol^{-1} for the binding energies

	σ	η^2 Planar	η^2 Pseudo-tetrahedral	η^3
E	−2227.9018	−2227.9029	−2227.9050	−2227.9009
b.e.*	−1.5	−2.2	−3.5	−1.0

* Referred to the metal fragment in the same geometry as in the *cis* optimized $[Ni(PH_3)_2(CH_3)H]$ complex.

of the C–H bonds of CH_4 with regard to the metal. Four geometrically different interaction modes of CH_4 with $Ni(PH_3)_2$ have been considered. The optimizations have been performed with strict symmetry constraints corresponding to σ, η^2 (planar or pseudo-tetrahedral) and η^3 complexes, *i.e.* complexes where the nickel atom interacts with one, two and three C–H bonds respectively (*cf.* ref. 35). For each complex we have optimized only one geometrical parameter, corresponding essentially to the Ni–C distance, using the optimized geometry for the CH_4 and a geometry corresponding to the optimized *cis*-planar $[Ni(PH_3)_2(CH_3)H]$ complex for the $Ni(PH_3)_2$ fragment. The structures obtained are reported in Fig. 3 together with the calculated values for the Ni–C and Ni–H distances. In Table 5 we report the SCF energies and the evaluated binding energies corresponding to these optimized structures. The binding energies have been computed as the differences between the energies of the complexes and the energies of the separated fragments. Since in computing these energies we have used partially optimized geometries for the complexes and non-optimized geometries for the nickel fragment, we expect our data to overestimate somewhat (in absolute value) the true fragmentation energies. However, this should not affect the main qualitative conclusions of our comparative analysis. We note that the most stable methane complex is the pseudo-tetrahedral η^2 one, with a binding energy of −3.5 kcal mol^{-1}. Note also its geometry with a Ni–C distance of 2.49 Å and a Ni–H distance of 2.07 Å (not shown in the Figure), both only about 0.5 Å longer than the bond values.

Strictly speaking, these stationary points are not necessarily true minima of the potential-energy surface, since the variation of unoptimized geometrical parameters could lower the energy. However, the effect of such variations is very small so that these stationary points can be considered as real complexes with possibly almost negligible geometrical corrections. For example, in the σ complex, the optimization of the C–H distance leads to a lengthening of 0.004 Å with an energy lowering of only less than 0.01 kcal mol^{-1}, and analogous effects can be predicted for the η^2 and η^3 complexes. When we considered the effect of a slight distortion of these complexes from their symmetric structures we found a small decrease in the σ complex and even an increase in the η^2 and η^3 one. In the former complex the optimization of the C–H–Ni angle, otherwise fixed at 180°, leads to an optimized angle of 155.0° and an energy lowering of about 0.2 kcal mol^{-1}. Thus, the only complex somewhat unstable with respect to the variation of other geometrical parameters seems to be the σ one, and the kind of variation reveals that the nickel centre tends to interact with the C–H more than with the H atom only.

In view of this fact we have performed a more complete geometry optimization of the σ complex taking into account the variation of the C–H bond length and of its orientation with respect both to the other three methane hydrogens and to the $Ni(PH_3)_2$ fragment. This optimization requires the variation of five geometrical parameters and has been performed in a planar arrangement, leading to the structure in Fig. 4 together with the optimized parameters. The resulting complex corresponds to a pseudo-side-on structure and has a binding energy of 2.3 kcal mol^{-1}.

The latter structure can be considered as a representative model of the so-called 'agostic' interaction between the metal centre and a single C–H bond.[3,14,15] The term 'agostic' has been proposed by Brookhart and Green[14] to indicate all the cases in which there is a covalent interaction between carbon–hydrogen groups and transition-metal centres in organometallic compounds. Interactions of this type have been known for more than twenty years, and much experimental evidence (mainly from neutron diffraction and NMR spectroscopy) has recently indicated that many complexes contain C–H • • • M bridges between a C–H bond of the ligand and the metal. These complexes have attracted much interest because they represent a plausible intermediate stage in the oxidative addition of C–H bonds to metal centres, so giving some information about the first stages of the reaction path leading to the transition state for such reaction. In all the known cases of complexes presenting relevant 'agostic' interactions the metal fragment has an electron-deficient electronic configuration. This is a clear indication that the interaction is due to a donation of the C–H bonding pair to the metal in a two-electron three-centre bond. The strength of the agostic interactions has been estimated to be as high as 20 kcal mol^{-1}, but it is usually lower falling in the range 5–10 kcal mol^{-1}. The dynamics of the C–H bond lengthening in the early stages of the oxidative addition of C–H bonds to metal centres has recently been studied by Crabtree *et al.*[16] by using the method of Burgi and Dunitz.[36] In this approach a succession of crystal structures for several complexes with different C–H to metal distances has been considered as frozen points of the reaction profile. As a measure of the C–H to metal distance the parameter r_{bp} has been used with $r_{bp} = d_{bp} - r_M$, d_{bp} being the distance between the metal and the C–H bonding pair (the point where carbon and hydrogen covalent radii meet) and r_M the covalent radius of the metal. The agostic interactions have been classified as weak for $r_{bp} > 1$ Å, strong for $r_{bp} < 0.7$ Å, and intermediate for $0.7 < r_{bp} < 1$ Å. The dependencies of both d_{CH} and MHC angle on r_{bp} have been reported for many experimental complexes with intramolecular agostic interactions and smooth curves could be drawn through them. Such dependencies suggest that the C–H bond is not significantly lengthened until $r_{bp} < 0.7$–0.8 Å and that the

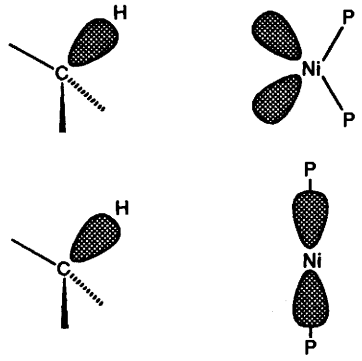

Fig. 5 Schematic representation of the interaction between the C–H bonding orbital and the lowest-unoccupied orbital of the $Ni(PH_3)_2$ fragment in the bent and linear geometries

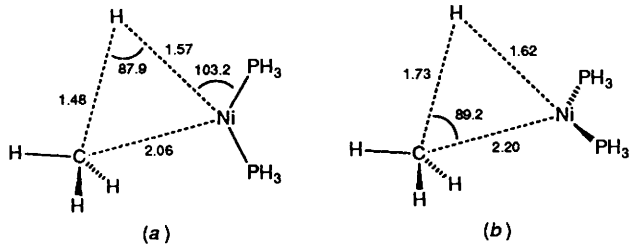

Fig. 6 Geometries of the transition states leading to the (*a*) *cis* and (*b*) *trans* oxidative-addition product. Bond lengths in Å, angles in °

Table 6 Total SCF and CI energies and corresponding activation energies (a.e.s) for the transition states connecting respectively the σ-methane complex with the *cis*-$[Ni(PH_3)_2(CH_3)H]$ complex, and the separated fragments approaching in a η^2-type configuration with the *trans*-$[Ni(PH_3)_2(CH_3)H]$ complex. The units used are Hartree for the total energies and kcal mol^{-1} for the activation energies

	σ ⟶ *cis*	η^2 type ⟶ *trans*
E_{SCF}	−2227.8746	−2227.8261
E_{CI}	−2228.5232	−2228.4750
$a.e._{SCF}$[a]	+34.4	+64.8
$a.e._{SCF}$[b]	+15.5	+64.8
$a.e._{CI}$[a]	+17.7	+47.9
$a.e._{CI}$[b]	−2.9	+47.9

[a] Referred to the metal fragment in the optimized linear geometry. [b] Referred to the metal fragment in the same geometry as in the corresponding optimized complex.

MHC angle is 130° at large r_{bp} and falls rapidly as r_{bp} decreases below 1 Å. Note that the limit is 130 and not 180° as would be consistent with the steric repulsion between the metal and the other groups on carbon. Although this effect could be due to the inability of the ligand structure to which the CH group is bound to achieve 180°, it has been ascribed to the most favourable interaction of both the d_σ metal orbital with the σ(C–H) orbital and the d_π orbital with the σ*(C–H) orbital (back donation).

It is interesting to see how our $Ni(PH_3)_2{\cdot}CH_4$ complex compares with the correlation of experimental data for complexes with intramolecular interactions, reported by Crabtree *et al.*[16] For the optimized structure of our complex we have r_{bp} = 1.04 Å with d_{CH} = 1.093 Å and Ni–H–C 128.6°, values which agree very well with the smooth curves reported in ref. 16. In the Crabtree *et al.*[16] scheme our complex would be classified as a weakly interacting case, as expected for a late transition metal, and confirmed by the 2.5 kcal mol^{-1} value for the binding energy. In particular the Ni–H–C angle agrees well with the limit value of 130° observed for all complexes with weak intramolecular agostic interactions and confirms the hypothesis that this value is due to electronic reasons rather than to ligand-structure constraints. Further support to this hypothesis is given by the bonding picture based on the analysis of the frontier orbitals for the optimized $Ni(PH_3)_2{\cdot}CH_4$ σ complex. The two highest-occupied orbitals show a mixing, although limited, between nickel d_{xy} and bonding σ(C–H) orbitals and between nickel $d_{x^2-y^2}$ and antibonding σ*(C–H) orbitals, respectively. The 128.6° Ni–H–C angle represents in this scheme the orientation which permits the maximum overlap of both the d_{xy} orbital and the H 1s and C sp^3 hybrid components of the σ(C–H) bonding orbital and the $d_{x^2-y^2}$ orbital with the components of the σ*(C–H) antibonding orbital. This aspect is somewhat confirmed by the analogous analysis in the linear complex (Ni–H–C 180°) which presents the two highest-occupied orbitals almost identical to those for the bent complex, as regards the nickel component, but with a much reduced mixing with the σ(C–H) and σ*(C–H) orbitals.

We have performed CI calculations on the σ-CH_4 complex at the SCF optimized geometry, to see the effect of the correlation on the agostic interaction. The results indicate again a stable complex with a slightly increased binding energy of 3.5 kcal mol^{-1}, probably underestimated since the minimum at the CI level does not necessarily coincide with that at the SCF level.

When the same partial geometry optimizations of the CH_4 + $Ni(PH_3)_2$ system, discussed above, are repeated using a fragment geometry corresponding to the energetically lowest *trans*-planar $[Ni(PH_3)_2(CH_3)H]$ complex (P–Ni–P essentially linear) no stationary point has been found, for all the σ, η^2 or η^3 approaching geometries. This different behaviour between bent and linear fragments may be ascribed to the different character of the highest molecular orbital: a d_{xy} nickel orbital well suited for interaction with the approaching C–H bond in the former case, and a d_{z^2} nickel orbital less suited for such an interaction in the latter case (see Fig. 5).

As a final step in our study of the potential-energy surface for the oxidative addition we have performed transition-state calculations in order to determine the geometries and the energies of the transition states connecting the lowest energy methane complexes with the lowest energy oxidative-addition products. We considered two different, geometry-constrained, reaction paths: the first one directly connects the σ-methane complex (see Fig. 4) with the $[Ni(PH_3)_2(CH_3)H]$ *cis*-planar complex (see Fig. 2); the second connects the separated fragments approaching in a η^2-type configuration with the $[Ni(PH_3)_2(CH_3)H]$ *trans*-planar complex (see Fig. 2). In both calculations we used the P–Ni–P angles obtained in the optimizations of the two *cis*- and *trans*-planar $[Ni(PH_3)_2(CH_3)H]$ complexes.

In the first calculation we have imposed that the axis of the breaking C–H bond lies in the fragment (P–Ni–P) plane, and optimized five coordinates: Ni–H and C–H distances, and three coplanar angles specifying the orientation of the breaking C–H bond and the methyl group with respect to the fragment. In the second calculation we imposed that the axis of the breaking C–H bond lies in the plane perpendicular to the fragment plane bisecting the P–Ni–P angle, and optimized four coordinates: Ni–C and breaking C–H distances, the Ni–C–H angle and another Ni–C–H angle (referred to a non-breaking C–H bond) specifying the orientation of the methyl group with respect to the fragment plane.

We determined two saddle points, whose corresponding transition-state geometries are reported in Fig. 6. The energies of these transition states and the activation energies for the corresponding reactions (leading directly to *cis*- and *trans*-planar oxidative-addition products, respectively) are reported in Table 6. It is interesting that, at the SCF level, the activation energy for the oxidative addition leading to the *trans* complex is much higher, 64.8 kcal mol^{-1}, than that for the *cis* complex, 34.4 kcal mol^{-1} (15.5 kcal mol^{-1} if referred to the bent fragment). This means that the *cis* isomer, thermodynamically less stable, is kinetically favoured over the *trans* one.

Among the geometrical features of the two transition states,

we note the long C–H distances (1.48 and 1.73 Å, for the *cis* and *trans* cases, respectively) and short (*i.e.* close to the values for the equilibrium structures) Ni–C and Ni–H distances, which indicate late transition states.

In order to analyse the effect of correlation on the activation energies we have performed SDCI calculations on the two transition states in the geometries determined at the SCF level. The results shown in Table 6 indicate that correlation considerably lowers the activation energies to +17.7 and +47.9 kcal mol^{-1}, respectively, for the *cis* and the *trans* isomers. Note that the activation energy for the path leading to the *cis* isomer is negative, −2.9 kcal mol^{-1}, if we refer to the bent fragment, *i.e.* the transition state connecting the σ-methane complex and the *cis* product is lower in energy than the separated $Ni(PH_3)_2$ + CH_4 fragments. Such a transition state presents, however, an energy barrier of +1.6 kcal mol^{-1} with respect to the σ-methane complex. Although with a certain degree of uncertainty (the transition-state geometry at the CI level could be different from that at the SCF level), this fact indicates that the reaction can take place without the dissociation of CH_4 from the nickel fragment, once the σ-methane complex is formed.

Conclusion

The *ab initio* study of the oxidative addition of CH_4 to $Ni(PH_3)_2$ has shown that such a reaction is endothermic by 7.0 kcal mol^{-1} and that the thermodynamically most favoured product is the planar *trans* isomer which is 3.4 kcal mol^{-1} more stable than the *cis* isomer. It has also shown that the generation mode and the geometry of the reacting fragment approaching the methane molecule has an important role.

The bonding picture confirms the usual qualitative interpretation of the C–H bond activation by metal centres through oxidative addition: a forward electron transfer from the bonding σ(C–H) orbital into empty metal orbitals and a backward electron transfer from occupied metal d orbitals into an antibonding σ*(C–H) orbital.

From a kinetic point of view, the *cis* isomer is favoured with an activation energy for the reaction path leading directly to it of +17.7 kcal mol^{-1}, 30.2 kcal mol^{-1} lower than that for the *trans* isomer.

Although the *ab initio* calculations show, as expected, a very weak binding mode of the methane to the metallic fragment, the relative energies for the σ, η^2 and η^3 approaching interactions are very informative for understanding the C–H bond activation.

Acknowledgements

The present work has been carried on within the Progetto Finalizzato CNR Materiali Speciali per Tecnologie Avanzate. One of us (N. R.) thanks IBM Semea for providing a fellowship.

References

1 J. Halpern, *Inorg. Chim. Acta*, 1985, **100**, 41.
2 M. Ephritikhine, *Nouv. J. Chim.*, 1986, **10**, 9.
3 R. H. Crabtree, *Chem. Rev.*, 1985, **85**, 245.
4 A. E. Shilov, *Activation of Saturated Hydrocarbons by Transition Metal Complexes*, D. Reidel, Hingham, MA, 1984.
5 *Selective Hydrocarbon Activation: Principles and Progress*, eds. J. A. Davies, P. L. Watson, A. Greenberg and J. F. Liebman, VCH, New York, 1990.
6 L. Vaska, *Acc. Chem. Res.*, 1968, **1**, 335.
7 G. W. Parshall, *Acc. Chem. Res.*, 1975, **8**, 113.
8 J. M. Buchanan, J. M. Stryker and R. G. Bergman, *J. Am. Chem. Soc.*, 1986, **108**, 1537.
9 R. A. Periana and R. G. Bergman, *J. Am. Chem. Soc.*, 1986, **108**, 7332.
10 M. Hackett and G. M. Whitesides, *J. Am. Chem. Soc.*, 1988, **110**, 1449.
11 W. D. Jones and F. J. Feher, *Acc. Chem. Res.*, 1989, **22**, 91.
12 A. D. Ryabov, *Chem. Rev.*, 1990, **90**, 403.
13 J. P. Colman and L. S. Hegedus, *Principles and Applications of Organotransition Metal Chemistry*, University Science Books, Mill Valley, CA, 1980.
14 M. Brookhart and M. L. H. Green, *J. Organomet. Chem.*, 1983, **250**, 395.
15 M. Brookhart, M. L. H. Green and Luet-Lok Wong, *Prog. Inorg. Chem.*, 1988, **31**, 1.
16 R. H. Crabtree, E. M. Holt, M. Lavin and S. M. Morehouse, *Inorg. Chem.*, 1985, **24**, 1986.
17 R. Ross, A. Veillard and G. Vinot, *Theor. Chim. Acta*, 1971, **20**, 1.
18 D. M. Hood, R. M. Pitzer and H. F. Schaeffer III, *J. Chem. Phys.*, 1979, **71**, 705.
19 A. K. Rappe, T. A. Smedley and W. A. Goddard III, *J. Chem. Phys.*, 1981, **85**, 2607.
20 Y. Sakai, H. Tatewaki and S. Huzinaga, *J. Comput. Chem.*, 1981, **2**, 100.
21 T. H. Dunning, jun., *J. Chem. Phys.*, 1970, **53**, 2853.
22 V. R. Saunders and J. H. Van Lenthe, *Mol. Phys.*, 1983, **48**, 923.
23 E. R. Davidson, in *The World of Quantum Chemistry*, eds. R. Daudel and B. Pullman, D. Reidel, Dordrecht, 1974.
24 M. F. Guest and P. Sherwood, *GAMESS User's Guide and Reference Manual*, SERC Daresbury Laboratory, 1990.
25 S. Sakaki, K. Kitaura and K. Morokuma, *Inorg. Chem.*, 1982, **21**, 760.
26 P. O. Widmark, B. O. Ross and P. E. M. Siegbahn, *J. Chem. Phys.*, 1985, **89**, 2180.
27 A. B. Rivers and R. F. Fenske, *J. Chem. Phys.*, 1981, **75**, 1293.
28 M. R. A. Blomberg, U. B. Brandemark, P. E. M. Siegbahn, K. B. Mathinsen and G. Karlstrom, *J. Chem. Phys.*, 1985, **89**, 2171.
29 S. D. Ittel and J. A. Ibers, *J. Organomet. Chem.*, 1973, **57**, 389.
30 E. Sutton, *Tables of Interatomic Distances and Configurations in Molecules and Ions*, The Chemical Society, London, 1958.
31 J. J. Low and W. A. Goddard III, *J. Am. Chem. Soc.*, 1984, **106**, 8321.
32 J. J. Low and W. A. Goddard III, *J. Am. Chem. Soc.*, 1986, **108**, 6114.
33 J. J. Low and W. A. Goddard III, *Organometallics.*, 1986, **5**, 609.
34 J. Obaura, K. Kitaura and K. Morokuma, *J. Am. Chem. Soc.*, 1984, **106**, 7482.
35 J. Y. Saillard and R. Hoffmann, *J. Am. Chem. Soc.*, 1984, **106**, 2006.
36 H. B. Burgi and J. D. Dunitz, *Acc. Chem. Res.*, 1983, **16**, 153.

Received 13*th January* 1992; *Paper* 2/00150K